Journal of Catalysis **193,** 96–102 (2000)
doi:10.1006/jcat.2000.2884, available online at http://www.idealibrary.com on IDEAL®

Hydrodesulfurization Studies with a Single-Layer Molybdenum Disulfide Catalyst

William P. Boone[2] and John G. Ekerdt[1]

Department of Chemical Engineering, The University of Texas at Austin, Austin, Texas 78712

Received December 2, 1999; revised March 24, 2000; accepted April 3, 2000

Alumina-supported single-layer MoS_2 was prepared and its hydrodesulfurization (HDS) activity compared to an alumina-supported multilayer MoS_2 catalyst. Single-layer crystallites were formed by exfoliation of lithium-intercalated 2H–MoS_2 crystals and were deposited on γ-alumina at pH 10.5–11. The single-layer material is shown to be stable under reaction conditions and catalytic with similar activity and selectivity relative to the multilayer catalyst in the HDS of thiophene and tetrahydrothiophene. © 2000 Academic Press

Key Words: **hydrodesulfurization; molybdenum disulfide; thiophene desulfurization; tetrahydrothiophene desulfurization; model catalyst for hydrodesulfurization.**

INTRODUCTION

Hydrodesulfurization (HDS) is a commercially important process where the incoming petroleum feed is treated with hydrogen to remove sulfur from the petroleum as hydrogen sulfide. With the exhaustion of many of the sweet crude oil sources rich in these light fractions and with the increased demand for fuels, heavier feedstocks must be used. While some of these heavy feedstocks contain as little as 0.5 wt% sulfur, most contain between 2 and 7 wt% sulfur before being processed. HDS performance is reduced for these heavy feedstocks because they contain a proportionally larger amount of thiophene and alkyl-substituted thiophene analogues, multiring compounds such as dibenzothiophene and alkyl-substituted dibenzothiophenes, which are the most difficult molecules to desulfurize (1). As the oil industry moves toward the use of heavier feedstocks and as society moves toward requirements for cleaner fuels, development of catalysts to efficiently desulfurize these molecules becomes critical.

Molybdenum disulfide promoted by cobalt and supported on γ-alumina is the most commonly used catalyst for HDS (2–6). Molybdenum disulfide exists as a trigonal prismatic crystal with distinct crystalline layers. Under reaction conditions, some of the bridging and terminal sulfur atoms at the edges of the crystal are lost, allowing access to the molybdenum atoms beneath and, as a result, the edge planes of the MoS_2 crystal are highly active in HDS (7, 8). Daage and Chianelli proposed their rim-edge model to explain differences in activity at the various perimeter Mo sites (7). The uppermost MoS_2 layer or rim sites are less sterically hindered than sites located on lower layers of the crystal, edge sites. Thus, molecules bound to rim sites have more freedom to assume nonlinear configurations than molecules bound to edge sites. Daage and Chianelli showed that hydrogenation of dibenzothiophene occurred only on the rim sites of MoS_2 crystallites, whereas HDS could occur on both rim and edge sites.

The catalyst support introduces the possibility of steric or electronic interactions between the crystallite and support that may affect HDS activity and selectivity. Single-layer crystallites of MoS_2 on alumina afford a model system to explore these support effects. Frindt and co-workers have proposed a novel scheme for the preparation of such a material (9–12). In this scheme, bulk MoS_2 powder is soaked in a solution of *n*-butyllithium in hexanes, allowing lithium to intercalate between the crystal layers. The Li-intercalated MoS_2 is then washed to remove excess *n*-butyllithium and dried to yield a powder. When deposited in water, the intercalated lithium reacts with water, releasing hydrogen gas between the crystal layers. The rapid volume change due to gas formation exfoliates the crystal layers. The result is a suspension of small, planar particles of single-layer MoS_2 in water. If the suspension is acidified, the single-layer MoS_2 particles will rapidly aggregate and precipitate from solution. The suspension as prepared is somewhat basic due to the presence of LiOH from the reaction of lithium with water; under these conditions, the particles will not aggregate and the suspension will last several weeks. Similar suspensions can be prepared using WS_2 and $LiBH_4$ to yield single-layer particles of WS_2 (13).

The addition of alumina powder to the suspension causes the single-layer MoS_2 particles to flocculate on the alumina.

[1] To whom correspondence should be addressed. Fax: (512) 471-7060. E-mail: ekerdt@che.utexas.edu.

[2] Current address: Ford Scientific Research Laboratories, P.O. Box 2053, Dearborn, MI 48121.

0021-9517/00 $35.00

Catalysts prepared by this method have been used for CO hydrogenation to methane (11). It should be possible to form almost exclusively single-layer crystallites of MoS_2 on the alumina surface by properly controlling the concentration of MoS_2 crystallites and the system pH. Yang and Frindt prepared samples of single-layer MoS_2 on alumina and claimed they contained less than 10% multilayer crystals on the basis of a weak diffraction peak at $(2 \sin \theta/\lambda)$ of 0.16 $Å^{-1}$ that they assigned as the (001) reflection (9). There is no (001) peak in the standard data files for 2H–MoS_2; the (002) reflection should be seen at $(2 \sin \theta/\lambda)$ of 0.163 $Å^{-1}$ (14). If the peak at $(2 \sin \theta/\lambda)$ of 0.16 $Å^{-1}$ is the (002) reflection, their sample contained multilayer material. Unfortunately, the percentage of multilayer material cannot be estimated from their data. Work with cobalt-decorated MoS_2 crystallites on alumina ("CoMoS") has shown two distinct forms of CoMoS phases (15). Type I CoMoS on alumina is believed to consist of single-layer crystallites and type II alumina-supported CoMoS consists of multilayer crystallites. Alumina-supported single-layer MoS_2 crystallites prepared by the procedure described above may provide a useful comparison to type I CoMoS.

Molybdenum disulfide crystallites supported on alumina have been prepared by thermal decomposition of $(NH_4)_2MoS_4$ (16). Thermal decomposition in helium at 523 K has been shown to produce MoS_x with excess sulfur present ($x > 2$). Reduction in hydrogen at 523 K has been shown to produce a sulfur-deficient MoS_x ($x < 2$). The latter form is consistent with the structure of MoS_2 under hydrodesulfurization conditions (8, 17, 18). X-ray diffraction (XRD) analysis indicated that the material formed was consistent with crystalline MoS_2. No detectable formation of Mo–O bonds was reported by this route.

This paper compares the HDS activity of single-layer MoS_2 and multilayer MoS_2 supported on γ-alumina. We report that the two materials have similar catalytic activity and selectivity in HDS of the model compounds thiophene and tetrahydrothiophene (THT).

METHODS

Preparation of Multilayer MoS_2

Alumina-supported MoS_2 was prepared by a method adapted from that of Vasudevan and Zhang. Three-tenths of a gram of $(NH_4)_2MoS_4$ (Aldrich, 99.97%) was dissolved in 20 g of deionized water. This solution was added to a sidearm tube containing 1.5 g of alumina (Davison alumina powder, 99%, 280 m^2/g; received as α-alumina monohydrate and converts to γ-alumina when the catalyst is annealed). The solution and support were mixed and purged with argon for 2 h. The water was then removed under reduced pressure at 295 K. The resulting orange solid is air-sensitive but is stable indefinitely under argon. Approximately 200 mg of this solid was used for each hydrodesulfurization experiment and was transferred to the reaction U-tube under argon. Removal of NH_4 and excess sulfur was accomplished by the sample being heated to 773 K in the presence of hydrogen immediately before the HDS experiment.

Preparation of Single-Layer MoS_2

Single-layer MoS_2 on alumina was prepared according to a method adapted from that of Frindt and co-workers (10). Sixty mg of MoS_2 was placed in one side of a double-tube recrystallizer. Approximately 20 ml of 1.6 M *n*-butyllithium solution in hexanes (Aldrich) was added by a double-tipped needle. The solution was stirred at 295 K for 72 h. The solid was allowed to settle and the liquid decanted to the other side of the recrystallizer. The solid was then washed with three portions of pentane (distilled over sodium and degassed 10 min with argon) and dried under argon. Fifty milliliters of deionized water was added and allowed to react for 10 min. The mixture was subjected to ultrasonication during this time. The liquid was then decanted into a beaker and allowed to sit overnight. The resulting suspension was opaque purple in color. Some solid material was observed on the bottom of the beaker.

One gram of alumina powder was placed in a Teflon beaker and 25 ml of deionized water added. The liquid suspension from above was drawn off the solid and added to the Teflon beaker with the alumina. The pH of the solution was adjusted to 11.0 (as measured by a pH meter) with either ~0.1 N HCl or ~0.1 N LiOH as needed. After the solution was stirred 1 h at 295 K, stirring was stopped and the mixture allowed to settle. The solution cleared rapidly (within 15 min) and a dark solid was observed. This solid was collected by vacuum filtration using MFS #2 filter paper, washed repeatedly with deionized water to remove LiOH, and allowed to dry in air overnight. The solid was then annealed at 573 K for 3 h in helium to generate the desired catalyst.

It should be noted that, at a pH above 11.5, the single-layer MoS_2 particles did not deposit on alumina after 2 days of stirring. Below pH 8.0 the particles deposited rapidly on alumina, but the XRD pattern showed the presence of the (002) reflection, indicating that multilayer MoS_2 was formed.

Characterization

Catalyst molybdenum content was determined by atomic absorption spectroscopy (AAS) using a Varian AA-1475 flame ionization spectrophotometer. Details of sample preparation and analysis are provided elsewhere (19). X-ray diffraction (XRD) was performed using a Philips PW 1729 X-ray generator using Cu $K\alpha$ X-rays ($\lambda = 1.5406$ Å) at 40 kV and 40 mA. A Philips APD 3520 was used to integrate

intensity (counts). A step size of 0.05° 2θ and a scan speed of 0.5° 2θ/min were used.

X-ray photoelectron spectra were collected using a Physical Electronics system with monochromatic Al $K\alpha$ X-rays (1486.7 eV) at a source power of 300 W. Chamber pressure during measurement was about 10^{-9} Torr. Samples were mounted by attachment of the powder to double-sided tape. Samples showing a Mo oxide signal (Mo(IV) oxides and the multilayer MoS_2 on alumina) were transferred from the sealed reaction vessel to the mount in a drybox to prevent oxygen contamination. Other samples were mounted in either a drybox or ambient air; no difference was observed in the spectra obtained. A neutralizer was used to minimize charging of the electrically insulating catalysts during data collection. Survey scans were usually taken over a range of 0–1400 eV with a step size of 0.4 eV for 200 ms/step and a pass energy of 94 eV. High-resolution scans of the molybdenum 3*d* and sulfur 2*p* regions were collected over a 20- or 30-eV range within the region of interest with a step size of 0.1 eV for 1000 ms/step and a pass energy of 12 eV being used. Binding energies were corrected for sample charging by translation of the data so that the C 1*s* peak (of adventitious carbon) was at 284.5 eV.

A Gaussian peak form was assumed when peaks were fitted to XP spectra. Relative peak areas were fixed at a 60 : 40 ratio for the Mo $3d_{5/2}/3d_{3/2}$ peaks. Full width at half height was allowed to vary but was assumed constant for each of the two peaks of the Mo $3d_{5/2}/3d_{3/2}$ pair. Peak heights and locations were permitted to vary. The optimization algorithm minimized the sum of the square of the difference between the observed signal and the sum of all component peak signals.

HDS reactions were performed and analyzed using a continuous-flow reactor previously described (20). The effluent gas from the reactor was analyzed on-line using a Hewlett-Packard 5890 gas chromatograph with a flame ionization detector. A 1-ml sample of the effluent gas was collected using an automatic sampling valve and injected onto a 50 m × 0.53 mm PLOT Al_2O_3/KCl column (Chrompak). The detector was calibrated using a 1010 ppm methane/1010 ppm propane/helium mixture (Matheson, certified). The relative sensitivity of the flame ionization detector was corrected using effective carbon numbers (21).

Thiophene (Janssen, 99+%) was purified by several freeze/pump/thaw cycles before use. Gas chromatography showed that total impurities were less than 0.25%. No detectable tetrahydrothiophene was observed. Thiophene was fed to the reactor system by hydrogen gas being passed at a flow of 18 ml/min through a saturator containing liquid thiophene at 295 K and 1 atm. This resulted in a feedstream of about 8.7% thiophene in hydrogen. The reactor temperature varied from 523 to 673 K.

Tetrahydrothiophene (Aldrich, 99%) was purified through several freeze/pump/thaw cycles before use. Gas chromatography confirmed that less than 0.25% impurities was present. No detectable thiophene was observed in the tetrahydrothiophene reactant. Tetrahydrothiophene was fed to the reactor system by hydrogen gas being flowed at 18 ml/min through a saturator system containing liquid tetrahydrothiophene at 295 K and 1 atm, resulting in a stream of about 1.9% tetrahydrothiophene in hydrogen. The reactor temperature was again varied from 523 to 673 K.

RESULTS AND DISCUSSION

X-ray diffraction was used to determine what crystalline phases were present in the molybdenum disulfide catalyst samples as well as whether the catalysts consisted of single-layer or multilayer crystals. Molybdenum disulfide exists primarily as a trigonal prismatic crystal with distinct crystalline layers. The X-ray diffraction pattern of bulk MoS_2 (Aldrich, 99%) is shown in Fig. 1. Three reflections are significant for the determination of whether a crystal is single layer or multilayer. The (100) and (110) reflections at 2θ of 32.7° and 58.3°, respectively, arise from reflections within a single layer and would be present in both single-layer and multilayer crystals. The other reflections shown, notably the intense (002) reflection at 2θ of 14.4°, arise from interactions between crystal layers and thus would only exist in multilayer crystals.

The crystallite size for the molybdenum disulfide catalyst was determined by X-ray line broadening. The peak width at half height of the (100) and (110) peaks was calculated by subtraction of the X-ray diffraction spectrum of the support heated under the same conditions as those used for preparation of the MoS_2 catalysts from that of the catalyst and fitting of the resulting peaks as Gaussian–Lorentzian. Approximate crystallite dimension parallel to the basal plane

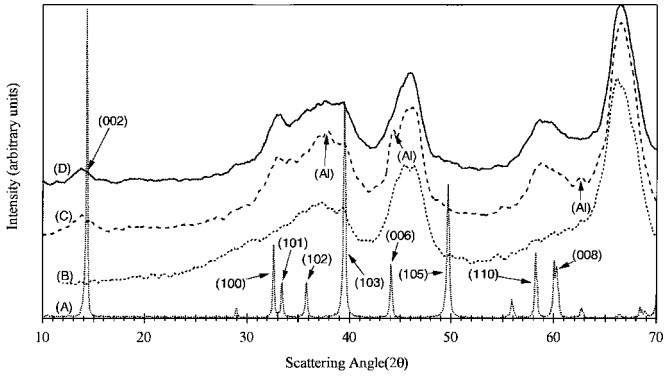

FIG. 1. XRD pattern of multilayer MoS_2 before and after reaction. Peaks labeled (Al) arise from the aluminum sample holder used, (A) bulk MoS_2, (B) alumina support heated under conditions of catalyst preparation, (C) as-prepared multilayer MoS_2 on alumina, and (D) multilayer catalyst on alumina after 12-h thiophene HDS at 773 K.

was determined from X-ray line broadening of the (100) and (110) reflections. Crystallite dimension perpendicular to the basal plane was determined from X-ray line broadening of the (002) reflection and, when present, the (008) reflection. The unit cell for molybdenum disulfide is hexagonal with dimensions of $a = 3.161$ Å and $c = 12.299$ Å and consists of two layers, each containing a single molybdenum atom (14). From these data, the total number of perimeter molybdenum atoms could be calculated. These calculations assume that all X-ray line broadening is due to crystal size. Defects have been shown to occur in MoS_2 crystallites (22) and may also contribute to X-ray line broadening. The calculations also assume that the crystallites are trigonal prismatic as those in bulk 2H–MoS_2. A recent preparation of MoS_2 crystallites on Au(111) from vapor-phase Mo and H_2S led to triangular crystallites (23). While such a reconstruction seems unlikely with the preparations described above, it is a possibility. Both of these issues may lead in errors in calculation of perimeter Mo atoms.

The X-ray diffraction pattern for the multilayer catalyst before and after HDS is shown in Fig. 1. The peaks are consistent with the presence of MoS_2 crystallites. There is no apparent change in crystallite size or shape after reaction. The presence of the (002) peak indicates that multiple layers of MoS_2 are present in the crystallites. X-ray line-broadening analysis suggests an average crystal size for MoS_2 of 75 ± 9 Å with a thickness of 26 Å for the alumina-based catalyst. This corresponds to a crystal four-layers thick with approximately 12.8% of the Mo atoms on the crystal edge.

The XRD pattern of the single-layer catalyst before and after HDS is shown in Fig. 2. The low weight loading of the catalyst and the small crystal size combine to make the XRD peaks broad and to be of low amplitude, and as a result they are difficult to see. The pattern shows reflections consistent with the (100) and (110) peaks of MoS_2, indicating the desired crystalline material has been formed. A small peak consistent with the (002) reflection can be seen in a catalyst prepared with 4.5 wt% Mo (Fig. 2, curve C), suggesting that some multilayer material is present for this weight loading. No trace of the (002) reflection can be seen on a similar catalyst with only 0.9 wt% Mo (Fig. 2, curves D and E). The (100) and (110) peaks are extremely broad and weak on this catalyst but can be assigned from the peaks observed on the 4.5 wt% Mo catalyst. Due to the broad nature of the MoS_2 peaks, it is not possible to conclusively say that the (110) peak does not contain the (008) peak as well; however, the (008) peak cannot be present if the (002) reflection is absent. Since there is no trace of the more intense (002) peak, it can be concluded that the (008) peak is absent as well. The equipment used is unlikely to detect crystallites smaller than 20 Å in size. Thus, a two- or three-layer crystallite (12.3 and 18.4 Å in height, respectively) would not show a (002) reflection, and it cannot be conclusively shown by the lack of the (002) reflection that the crystallites are single layer. Samples prepared by Frindt using the exfoliation method have XRD patterns similar to theoretical ones calculated for single-layer crystallites (9); these crystallites do show a small (002) peak, indicating the presence of some multilayer material. The crystallites prepared for the study reported herein are likely to contain some multilayer material as well. However, the "single-layer" samples in this study much more closely resemble true single-layer crystallites than the multilayer samples prepared from $(NH_4)_2MoS_4$. X-ray line-broadening analysis of the 0.9 wt% Mo material leads to a calculation of an average crystal size of 130 ± 15 Å, indicating that approximately 7.3% of the Mo atoms are on the crystal edge.

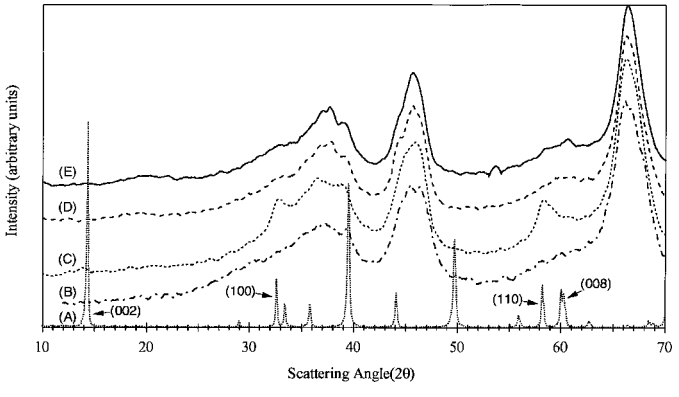

FIG. 2. XRD pattern of single-layer MoS_2 before and after reaction: (A) bulk MoS_2, (B) alumina support heated under conditions of catalyst preparation, (C) as-prepared single-layer MoS_2 with 4.5 wt% Mo, (D) as-prepared single-layer MoS_2 with 0.9 wt% Mo, and (E) 0.9 wt% Mo single-layer catalyst after 12-h thiophene HDS at 773 K.

X-ray photoelectron spectroscopy was used to confirm that all Mo atoms were in the correct oxidation state. The XP spectrum of the multilayer catalyst as prepared is shown in Fig. 3. This material shows peaks for the Mo $3d_{5/2}$ and Mo $3d_{3/2}$ at 228.1 and 231.3 eV, respectively. The sulfur 2*p* peak (not shown) appears at 161.8 eV. These values are typical of those for MoS_2 (24, 25). A second set of peaks was observed at 232.2 and 235.4 eV. These peaks are consistent with a Mo(IV) oxide prepared from cyclopentadienylmolybdenumtricarbonyl dimer, $(CpMo(CO)_3)_2$ (19). The peaks likely arise from the presence of amorphous Mo(IV) oxide in the sample. Figure 4 shows the XP spectra of the multilayer catalyst before and after HDS. The peaks arising from Mo(IV) oxide disappear after the reaction. This suggests that the Mo(IV) oxide is located at the edges of the crystals and is rapidly sulfided under HDS conditions.

The XP spectrum of the 0.9 wt% Mo single-layer catalyst before and after reaction is shown in Fig. 5. Analysis shows Mo $3d_{5/2}$ and $3d_{3/2}$ peaks at 228.1 and 231.0 eV and sulfur 2*p* at 161.8 eV. As noted for the multilayer catalysts above, these values are consistent with MoS_2. A shoulder can be

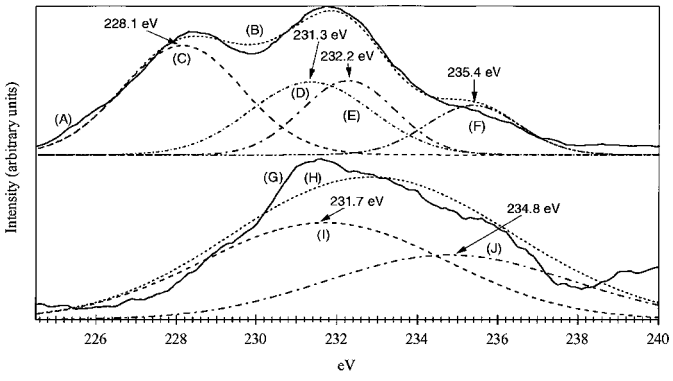

FIG. 3. Comparison of XP spectra of as-prepared multilayer MoS_2 and a Mo(IV) oxide prepared from $(CpMo(CO)_3)_2$: (A) XP spectrum for multilayer MoS_2, (B) total curve fit to MoS_2 XP spectrum, (C) MoS_2 $3d_{5/2}$, (D) MoS_2 $3d_{3/2}$, (E) believed Mo(IV) oxide $3d_{5/2}$, (F) believed Mo(IV) oxide $3d_{3/2}$, (G) XP spectrum for Mo(IV) oxide from $(CpMo(CO)_3)_2$, (H) total curve fit to Mo(IV) oxide XP spectrum, (I) Mo(IV) oxide $3d_{5/2}$, and (J) Mo(IV) oxide $3d_{3/2}$.

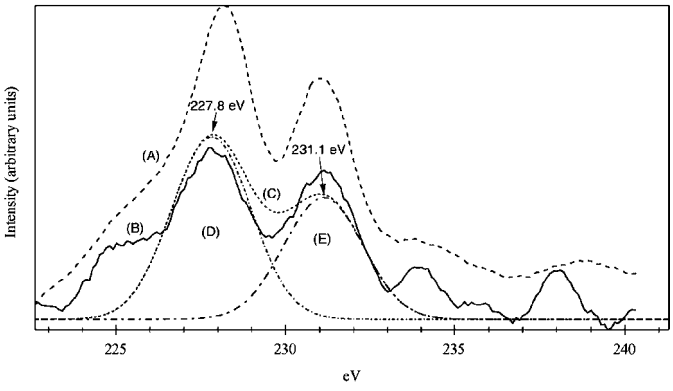

FIG. 5. Comparison of XP spectra of 0.9 wt% Mo single-layer MoS_2 before and after reaction: (A) XP spectrum of MoS_2 before reaction, (B) XP spectrum of MoS_2 after reaction, (C) total curve fit to after-reaction XP spectrum, (D) MoS_2 $3d_{5/2}$, and (E) MoS_2 $3d_{3/2}$.

seen on the $3d_{5/2}$ peak at about 225 eV; however, no form of Mo appears in this region of the spectrum. Similarly, small peaks can be seen at 234 and 238 eV. Due to the low weight loading of Mo on this catalyst and the likely buildup of carbonaceous material during the HDS reaction, the XP signal is extremely weak. It is probable that the shoulder and additional peaks are artifacts of baseline noise from this weak signal, but this cannot be confirmed.

Figure 6 plots the rate of production of HDS reaction products with time for the reaction of thiophene over single-layer MoS_2 at 523 K. The steady-state product rate is typical of reactions over the single-layer and multilayer MoS_2 catalysts at all temperatures studied. There is essentially no induction time, as is expected since the preparation generates molybdenum sulfide in the correct oxidation state (Fig. 5). Assuming that all Mo is available for reaction, turnover numbers (TONs) for multilayer and single-layer MoS_2 after 12 h of reaction at 773 K with thiophene were 35.6 and 14.9, respectively. As noted above, HDS is believed to occur at the edge of the MoS_2 crystallites (7, 8). Assuming that only edge Mo atoms are available for reaction, the TONs for the multilayer and single-layer catalyst become 278 and 204, respectively. These TONs conclusively show that the single-layer material is catalytic for HDS. Furthermore, the similarity of the TONs once corrected for the amount of Mo on the crystal edge indicates that there is little difference in the activity of the single-layer and multilayer catalysts.

Tables 1 and 2 show the relative product distributions for thiophene and THT HDS, respectively, with the multilayer and single-layer MoS_2 catalysts at 673 K. (The high reaction temperature was chosen to increase reaction

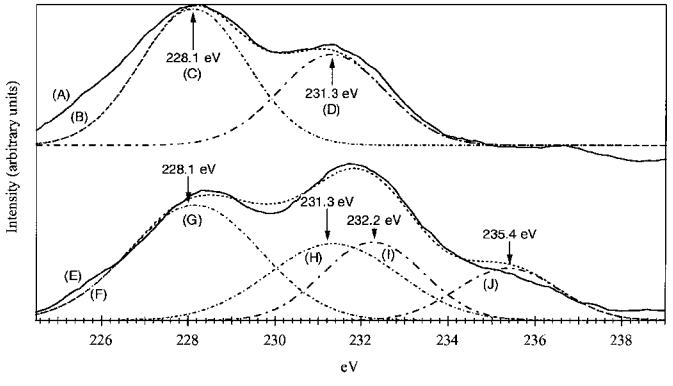

FIG. 4. Comparison of XP spectra of multilayer MoS_2 before and after reaction: (A) XP spectrum of MoS_2 after reaction, (B) total curve fit to after-reaction XP spectrum, (C) MoS_2 $3d_{5/2}$, (D) MoS_2 $3d_{3/2}$, (E) XP spectrum of MoS_2 before reaction, (F) total curve fit to before-reaction XP spectrum, (G) MoS_2 $3d_{5/2}$, (H) MoS_2 $3d_{3/2}$, (I) Mo(IV) oxide $3d_{5/2}$, and (J) Mo(IV) oxide $3d_{3/2}$.

TABLE 1

Relative Product Distribution for Thiophene HDS at 673 K

	Multilayer MoS_2/ alumina 2.7 wt% Mo	Single-layer MoS_2/ alumina 0.9 wt% Mo
C1–C3 products[a]	5.82	8.66
i-Butane	0.29	0[c]
n-Butane	16.15	5.85
trans-2-Butene + 1-butene[b]	51.23	60.52
i-Butene	0.44	0[c]
cis-2-Butene	25.5	18.2
Butadiene	0.56	6.77

[a] C1–C3 products are combined because none are present in more than small quantities.

[b] *trans*-2-Butene and 1-butene are reported as a combined value because the two products separated poorly and incompletely in analysis.

[c] Values reported as zero are below the detection threshold.

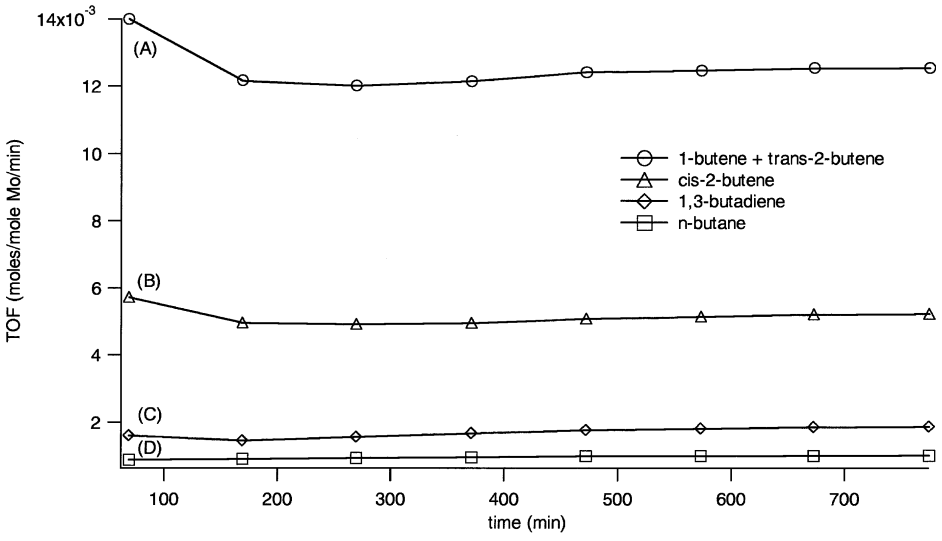

FIG. 6. Production rates for major reaction products in HDS of thiophene over 0.9 wt% Mo single-layer MoS_2 at 773 K: (A) 1-butene and *trans*-2-butene, (B) *cis*-2-butene, (C) 1,3-butadiene, and (D) *n*-butane.

rates and to allow detection of minor products.) The product distributions given in Tables 1 and 2 are typical of those at other HDS temperatures in this study. The most notable difference in the reaction product distribution is the formation of a higher percentage of unsaturated products (butadiene and butenes) with the single-layer catalyst. Butadiene, which is rapidly hydrogenated to butane and butenes under reaction conditions, is a primary product of thiophene and THT HDS (26). The single-layer catalyst has a much lower weight loading of Mo than the multilayer catalyst. Test runs on a single-layer catalyst with approximately the same weight loading as the multilayer catalyst gave product distributions essentially identical to those for the multilayer catalyst given in Tables 1 and 2. Thus, the higher percentage of unsaturated products is likely due to less hydrogenation of butadiene produced and not a fundamental difference in the primary HDS products generated. The similar activities and primary product distributions of the single-layer and multilayer catalyst suggest that the rim and edge sites of these two catalysts have similar capabilities for both hydrogenation and HDS of the small sulfur-containing molecules used.

Arrhenius plots for thiophene and THT HDS with the two catalysts are given in Fig. 7. (For clarity, error bars

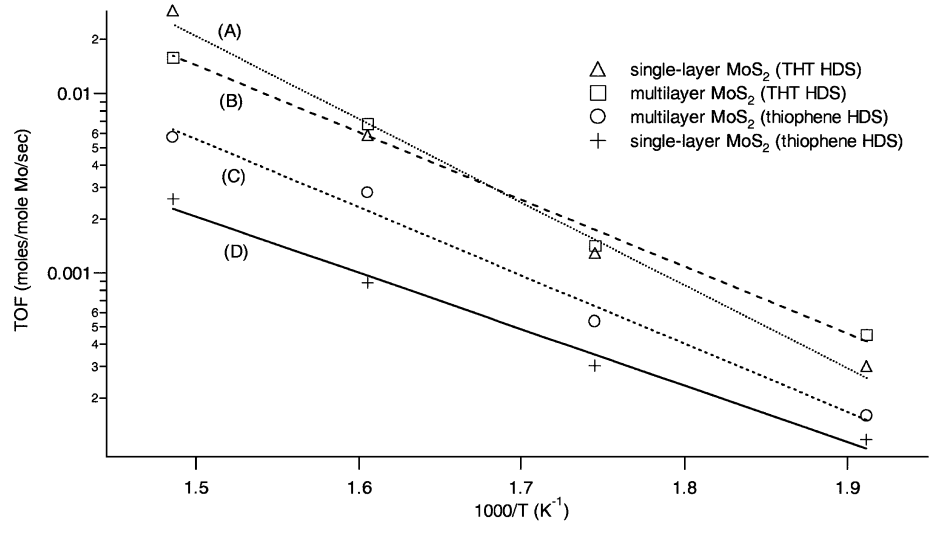

FIG. 7. Arrhenius plots for thiophene and THT HDS with MoS_2 catalysts: (A) 0.9 wt% Mo single-layer MoS_2 for THT HDS, (B) multilayer MoS_2 for THT HDS, (C) multilayer MoS_2 for thiophene HDS, and (D) 0.9 wt% Mo single-layer MoS_2 for thiophene HDS.

TABLE 2

Relative Product Distribution for THT HDS at 673 K

	Multilayer MoS_2/ alumina 2.7 wt% Mo	Single-layer MoS_2/ alumina 0.9 wt% Mo
C1–C3 products[a]	7.11	8.17
i-Butane	0.35	0.02
n-Butane	26.1	5.22
trans-2-Butene + 1-butene[b]	44.73	55.11
i-Butene	0.37	0[c]
cis-2-Butene	21.02	18.29
Butadiene	0.33	13.2

[a] C1–C3 products are combined because none are present in more than small quantities.

[b] trans-2-Butene and 1-butene are reported as a combined value because the two products separated poorly and incompletely in analysis.

[c] Values reported as zero are below the detection threshold.

have been omitted; however, TOFs given are accurate to about ±10%.) HDS reactions were performed in the temperature range 523–673 K. Apparent activation energies of the MoS_2 catalysts for thiophene HDS were calculated as 72.8 and 60.2 kJ/mol for multilayer and single-layer MoS_2, respectively. Apparent activation energies for THT HDS were determined as 71.6 and 88.6 kJ/mol for single-layer MoS_2, respectively. The similarity of these values within experimental error underscores the above observations that there is little difference in the activity of the single-layer and multilayer catalysts. This is consistent with previous work that shows little difference in HDS activity between type I and type II alumina-supported CoMoS (15).

In summary, single-layer MoS_2 is a catalytic material for thiophene and THT HDS and is similar in both activity and selectivity to multilayer MoS_2 catalysts. The single-layer catalyst showed a significantly higher percentage of unsaturated products relative to the multilayer catalyst. This is due to a decrease in the hydrogenation of the butadiene initially produced because of the low weight loading of the single-layer catalyst. Further research is necessary to determine if the similarity of the single-layer and multilayer catalysts extends to the hydrodesulfurization of larger molecules such as dibenzothiophene.

ACKNOWLEDGMENT

This work was supported by a grant from the U.S. Department of Energy, Office of Basic Energy Sciences (Grant DE-FG03-95ER14570).

REFERENCES

1. Girgis, M. J., and Gates, B. C., *Ind. Eng. Chem. Res.* **30**, 2021 (1991).
2. Grange, P., *Catal Rev.-Sci. Eng.* **21**, 135 (1980).
3. Prins, R., de Beer, V. H. J., and Somorjai, G. A., *Catal. Rev.-Sci. Eng.* **31**, 1 (1989).
4. Ratnasamy, P., and Sivasanker, S., *Catal. Rev.-Sci. Eng.* **22**, 401 (1980).
5. Topsøe, H., and Clausen, B. S., *Catal. Rev.-Sci. Eng.* **26**, 395 (1984).
6. Chianelli, R. R., *Catal. Rev.-Sci. Eng.* **26**, 361 (1984).
7. Daage, M., and Chianelli, R. R., *J. Catal.* **149**, 414 (1994).
8. Drew, M. G. B., Mitchell, P. C. H., and Kasztelan, S., *J. Chem. Soc. Faraday Trans.* **86**, 697 (1990).
9. Yang, D., and Frindt, R. F., *in* "Symposium on Advances in Hydrotreating Catalysts, Washington, DC, Aug. 1994," p. 612. Div. of Petrol. Chem., Amer. Chem. Soc., Washington, DC, 1994.
10. Joenson, P., Frindt, R. F., and Morrison, S. R., *Mater. Res. Bull.* **21**, 457 (1986).
11. Miremadi, B. K., and Morrison, S. R., *J. Catal.* **103**, 334 (1987).
12. Divigalpitiya, W. M. R., Morrison, S. R., and Frindt, R. F., *Thin Solid Films* **186**, 177 (1990).
13. Tsai, H.-L., Heising, J., Schindler, J. L., Kannewurf, C. R., and Kanatzidis, M. G., *Chem. Mater.* **9**, 879 (1992).
14. JCPDS Powder Diffraction File, Sets 1–47, 1997.
15. Bouwens, S. M. A., van Zon, F. E. M., van Dijk, M. P., van der Kraan, A. M., de Beer, V. H. J., van Veen, J. A. R., and Koningsberger, D. C., *J. Catal.* **146**, 375 (1994).
16. Vasudevan, P. T., and Zhang, F., *Appl. Catal. A* **112**, 161 (1994).
17. Salmeron, M., Somorjai, G. A., Wold, A., Chianelli, R. R., and Liang, K. S., *Chem. Phys. Lett.* **90**, 105 (1982).
18. Farias, M. H., Gellman, A. J., Somorjai, G. A., Chianelli, R. R., and Liang, K. S., *Surf. Sci.* **140**, 181 (1984).
19. Boone, W. P., M. S. thesis, The University of Texas at Austin, 1999.
20. Sullivan, D. L., and Ekerdt, J. G., *J. Catal.* **172**, 64 (1997).
21. Sternberg, J. C., Gallaway, W. S., and Jones, D. T. L., *in* "Gas Chromatography" (N. Brenner, J. E. Callen, and M. D. Weiss, Eds.), p. 231. Academic Press, New York, 1962.
22. Shido, T., and Prins, R., *J. Phys. Chem. B* **102**, 8426 (1998).
23. Helveg, S., Lauritsen, J. V., Lægsgaard, E., Stensgaard, I., Nørskov, J. K., Clausen, B. S., Topsøe, H., and Besenbacher, F., *Phys. Rev. Lett.* **84**, 951 (2000).
24. Patterson, T. A., Carver, J. C., Leyden, D. E., and Hercules, D. M., *J. Phys. Chem.* **80**, 1700 (1976).
25. Chastain, J., Ed. "Handbook of X-Ray Photoelectron Spectroscopy." Perkin–Elmer Corp., Eden Prairie, MN, 1992.
26. Sullivan, D. L., and Ekerdt, J. G., *J. Catal.* **178**, 226 (1998).